

---

# Demographics of Molecular Cloud Evolution and Cluster Formation

---

PETER J. BARNES<sup>1</sup>, ERIK MULLER<sup>2</sup>, AUDRA K. HERNANDEZ<sup>3</sup>

PJB@UFL.EDU

<sup>1</sup> *Astronomy Department, University of Florida, Gainesville FL, USA*, <sup>2</sup> *National Astronomical Observatory of Japan, Mitaka, Japan*, <sup>3</sup> *Astronomy Department, University of Wisconsin, Madison WI, USA*

## Abstract

New multi-line mapping surveys of molecular clouds (e.g., CHaMP, ThrUMMS), are enabling an unprecedented demographic analysis of the physics of entire cloud populations. Key insights from such surveys include (but are not limited to): (1) The existence of a vast population of sub-thermally excited, massive dense clumps, the majority of which are not engaged in vigorous star formation; (2) The pressure-stabilisation of these clumps against dispersal by their overlying envelopes, implying long (several  $\times 10^7$  yr) cloud lifetimes; (3) A new CO  $\rightarrow$  H<sub>2</sub> conversion law accounting for these numerous pc-scale, low-excitation, high-opacity and high column density clumps, suggesting the total molecular mass of clouds, from pc to kpc scales in the Milky Way, may be underestimated by a factor of 2–3, and increasing the gas depletion timescale by the same factor; and (4) A revision to the concept of large molecular clouds, including GMCs, to be structures composed of pc-scale clumps ( $\sim 75\%$  by mass) connected by a more diffuse, large-scale envelope ( $\sim 25\%$  by mass). We summarise these results and discuss implications for our understanding of star formation and the life cycle of molecular clouds.

## 1. Motivation and Survey Landscape

Continuum surveys of cold, dusty gas, the raw material for star formation (e.g., GLIMPSE (1), Hi-GAL (2), ATLASGAL (3)), provide many new insights into this fundamental process and characterise well the mass, luminosity, temperature, and spectral energy distribution (SED, mostly from dust) in star forming clouds. However, crucial kinematic information from equivalent, sub-arcminute molecular-line mapping surveys is rare. **Key point 1:** at a typical distance of 3 kpc, 1' resolution corresponds to a scale of 1 pc, the threshold required to resolve cloud evolution on the scale of cluster formation (“clumps”), the Milky Way’s dominant mode of star formation (4).

So even the venerable CfA <sup>12</sup>CO survey (5) of Galactic GMCs cannot tell us much about clump evolution and formation of individual clusters. While the <sup>13</sup>CO GRS (6) can (resolution 0.8'), such surveys map only 1 species. Inherent chemical, thermodynamic, radia-

tive, or kinematic biases cannot be isolated, and our physical knowledge remains incomplete. **Key point 2:** progress in understanding clump physics and evolution *requires* a multi-species or multi-transition mapping strategy.

In this context, a few large-scale, multi-species spectroscopic mapping surveys stand out: CHaMP (7) (HCO<sup>+</sup>, HCN, N<sub>2</sub>H<sup>+</sup>, HNC, CN, 3 CO isotopologues: 0.6' resolution), MALT90 (8) (HCO<sup>+</sup>, HCN, N<sub>2</sub>H<sup>+</sup>, HNC: 0.6'), ThrUMMS (9) (iso-CO, CN: 1.2'), SEDIGISM (10) (<sup>13</sup>CO, C<sup>18</sup>O: 0.5') and now FUGIN (11) (iso-CO: 0.3'). These allow previously unfeasible *demographic* analyses of populations of cluster-forming molecular clumps: basic, physical parameters (column density, abundance ratios, etc.), that are otherwise inaccessible to existing, single-transition surveys.

## 2. First Demographic Results with CHaMP

Target selection for the CHaMP sample of molecular clumps (7) was based on the lower-resolution, complete, multi-transition Nanten survey (12) of a 20° $\times$ 6° sector of the Galactic Plane covering Vela, Carina, and Centaurus. It provides a complete population of 303 massive, dense clumps suitable for demographic analyses, and gave us the first new clues to the molecular cloud life cycle. In 2011, we confirmed (Fig. 1a) a prediction (13) from 2008 of a “vast population of subthermally-excited clouds,” based on a theoretical radiative transfer study of molecular lines in galactic disks.

The sub-thermal excitation also implies larger opacities and masses for these clouds than if one assumes thermalisation to (e.g.) dust/SED-derived temperatures. The large population showing little star formation activity implies either (a) long, quiescent lifetimes (50–100 Myr) for clumps before they form stars (*requires pressure-stabilisation*), or (b) a high creation/destruction rate (*requires ephemeral clouds*). These are points to which we return below.

## 3. ThrUMMS Line Ratios

In the 120 deg<sup>2</sup> of the 4th Quadrant mapped by ThrUMMS (9), we see widespread variations in the

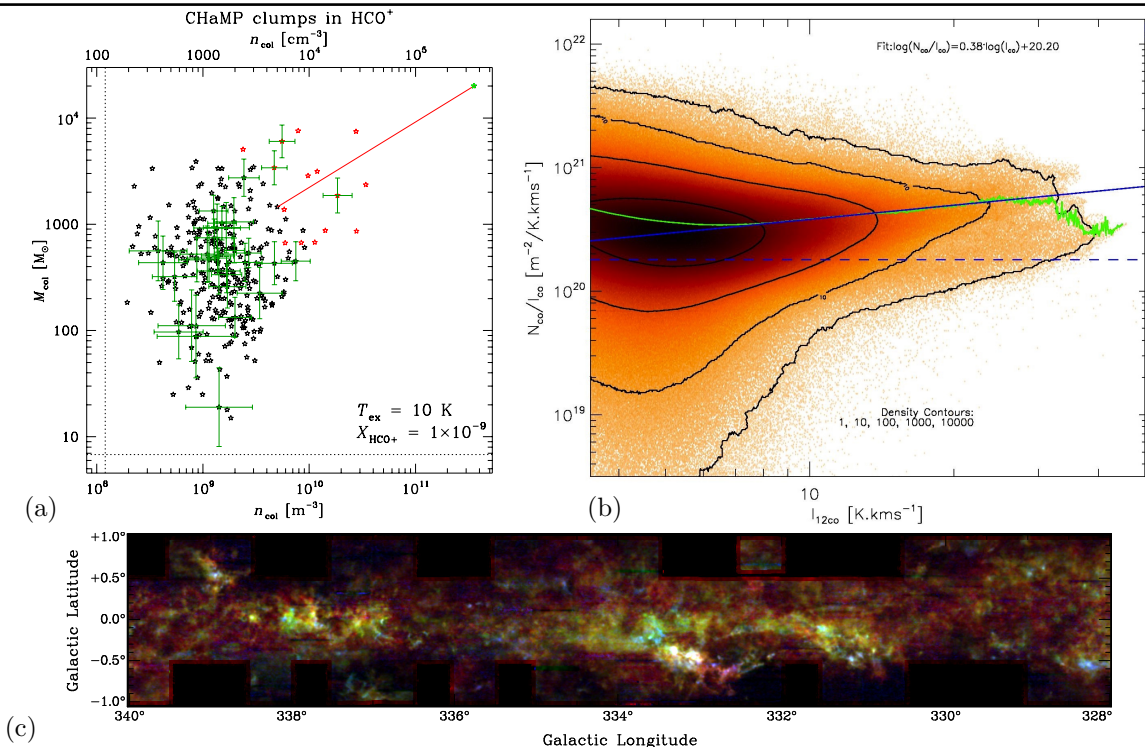


Figure 1. (a) CHaMP clumps’ mass vs density, as traced in HCO<sup>+</sup> emission (7). Red points are for the small fraction of clumps undergoing vigorous star formation; black points are for clumps that are either completely quiescent, or showing only minor star formation activity. Most of these are massive (several hundred  $M_{\odot}$  or more) yet below the critical density for the HCO<sup>+</sup> line, at  $\sim 2 \times 10^4 \text{ cm}^{-3}$ . The red line shows the opacity-corrected point for BYF 73, the only clump undergoing global contraction. (b) ThrUMMS  $N/I = X$  vs  $I$  data (9). The blue line shows the best power-law fit, which is not flat. (c) Sample three-colour image of ThrUMMS integrated intensity data (red = <sup>12</sup>CO, green = <sup>13</sup>CO, blue = C<sup>18</sup>O).

iso-CO line ratios, both on large (kpc) and small (pc) scales, and in the velocity dimension as well (Fig. 1c). Multi-species maps of individual clouds have revealed such variations before, but never on such a wide scale. The implications are enormous: e.g., based solely on the variable contrast between the <sup>12</sup>CO and the other species, it means that the concept of a standard  $X$  factor (i.e., “converting” <sup>12</sup>CO line intensity  $I$  to H<sub>2</sub> column density  $N$ ) is in grave jeopardy.

From the ThrUMMS cubes and line ratios, we obtained self-consistent plane-parallel radiative transfer solutions for the excitation temperature  $T_{\text{ex}}$ , optical depth  $\tau$ , and column density  $N$  across all  $10^9$  voxels of the survey (i.e., in 3D PPV space) and in each species. We found that areas where <sup>12</sup>CO is much brighter than <sup>13</sup>CO or C<sup>18</sup>O usually signify both a high excitation and low opacity for the CO-bearing gas. In contrast, areas where the 3 species are of comparable brightness usually signify low excitation and high opacity.

In terms of column density, the latter effect is stronger. For example, we also computed values for the 3D  $N/I$  ratio, which is effectively the much-discussed  $X$  factor (Fig. 1b). Instead of a linear relation, we obtained (9) a power-law fit  $N \propto I^{1.4}$ , giving a global average for  $X$

2–3 $\times$  higher than the standard value, mostly because the high-opacity clouds we found are not properly allowed for in other studies. This also suggests that molecular gas Kennicutt-Schmidt laws for disk galaxies may need to be recalibrated: e.g., the Milky Way’s molecular gas depletion timescale may be 2–3 $\times$  longer than previously thought, perhaps 5 Gyr instead of 2 Gyr.

#### 4. “Dense Gas” Tracers

Such indications of previously unrecognised large reservoirs of molecular gas are not limited to iso-CO results. HCN is a canonical “dense gas” tracer, with the advantage that its emission lines have hyperfine components which allow a similar radiative transfer calculation. We have a large sample of HCN maps from CHaMP, and have performed such an analysis on one cloud (14), with the rest of the sample being processed.

We find a similar result in the conversion of  $I$  to  $N$  for this species as well (Fig. 2a), namely that there is approximately twice as much gas as a simple  $I$ – $N$  conversion would suggest, and this gas resides in a low-excitation, high opacity reservoir not obviously

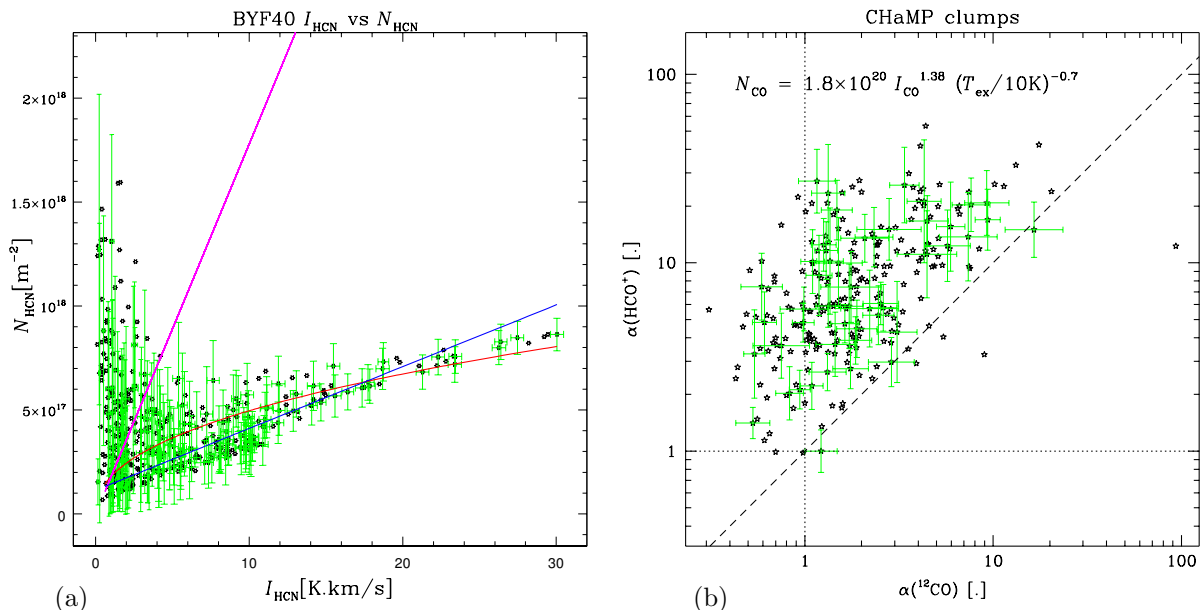


Figure 2. (a) HCN column density  $N$  vs integrated intensity  $I$ , from a pixel-by-pixel radiative transfer analysis of hyperfine components in one CHaMP cloud (14). The distribution of points cannot be fit with any simple linear or power law (coloured lines), and is a consequence of the highly non-linear relationship between the line brightness,  $T_{ex}$ , and  $\tau$ . (b) CHaMP clumps’ virial  $\alpha$ s as measured in both  $^{12}\text{CO}$  and  $\text{HCO}^+$  emission (16). The lower average value for  $^{12}\text{CO}$  arises from the molecule being so easy to excite, and thus able to trace lower densities than  $\text{HCO}^+$ , which then integrates to a higher mass. The  $\text{HCO}^+$  is, by comparison, sensitive only to the denser clump interior, and so underestimates the total clump mass that contributes to its confinement.

engaged in vigorous star formation. We also find that the HCN emission is extremely well-correlated with  $\text{HCO}^+$  emission, but not with  $\text{N}_2\text{H}^+$  emission. This is similar to the result from a near-IR emission line study of the CHaMP clouds (15), where  $\text{Br}\gamma$  is well-correlated with  $\text{HCO}^+$  emission, but not with  $\text{N}_2\text{H}^+$  emission. In combination, these results strongly suggest that neither  $\text{HCO}^+$  nor HCN emission truly trace dense gas, but are rather *post-star formation feedback indicators*, since they really trace a combination of column density weighted by excitation.

## 5. Demographics of Clump Envelopes

We recently completed a  $^{12}\text{CO}$  study (16) of the embedding envelopes of the massive, dense clump sample in CHaMP. Morphologically and dynamically, the clumps look very similar in the two tracers, despite the very different opacities (a factor of  $\sim 10^{2-3}$ ). However, because of the much lower effective density, the mass traced by  $^{12}\text{CO}$  emission is typically several times that traced by  $\text{HCO}^+$ . Since the clumps’ measured sizes and linewidths in these two tracers are similar, this means that the clumps’ measured virial  $\alpha$  ( $= 5\sigma^2 R/GM$ ) distribution has a mean of 2 in  $^{12}\text{CO}$ , compared to a mean of 8 in  $\text{HCO}^+$  (Fig. 2b).

We interpret this result as direct evidence for pressure-confinement of (at least half of) the population of massive dense clumps in the Milky Way. This means that, of the two scenarios for clump lifetimes suggested by the vast numbers of quiescent clumps (§2), the long-lifetime one is favoured. We also find that the clumps comprise approximately 75% of the total mass of all molecular clouds, from  $\sim 10$  pc to GMC scales, with only 25% of the mass lying in a lower-density intra-clump medium. These results should revise our picture of how mass is assembled in molecular clouds, before star formation can begin.

## 6. Reflections and Next Steps

One of the first results from SEDIGISM (10) confirms the basic physics underlying the ThrUMMS conversion law, through an analysis of the  $^{13}\text{CO}$   $J=2\rightarrow 1/J=1\rightarrow 0$  line ratio. This also demonstrates that the importance of high opacity/low excitation gas has been underestimated in molecular gas mass estimates, to the degree that we can obtain a close agreement between dust/SED-derived, and  $^{13}\text{CO}$ -derived, mass estimates. Thus, averaged across the  $1.5^\circ \times 1^\circ$  Test Field, any “CO-dark” gas seems to contribute relatively little to the mass budget.

Such key insights have only been possible with the multi-line spectroscopic mapping described here. Our new molecular cloud evolutionary paradigm seems to require a long latency period, several 10s of Myr, for the slow assembly of mass into (mostly) pc-scale, pressure-stabilised clumps, before a density threshold around  $10^4 \text{ cm}^{-3}$  is reached and vigorous star and cluster formation can begin, which then soon terminates clump evolution. During this process, much of the molecular gas has quite low excitation, and while detectable, is not traced by bright emission; the latter seems rather to indicate post-SF feedback.

We will continue to further test theory and “conventional wisdoms” with these rich survey resources, via new data releases, catalogues, multi-survey emission line analysis at mm and IR wavelengths, SED analysis of dust properties from  $\mu\text{m}$  to mm, and kinematic and dynamic studies from pc to kpc scales.

## Acknowledgments

We are indebted to many colleagues and students for their contributions to these survey projects, and without whom many of these results would have been far more difficult, or impossible, to obtain. We acknowledge support from grants NSF AST-1312597 and NASA ADAP-NNX15AF64G to PJB, and AST-1517573 to AKH.

## References

- [1] Benjamin, R. A., Churchwell, E., Babler, B. L., *et al*, *PASP* **115** 953 (2003).
- [2] Molinari, S., Swinyard, B., Bally, J., *et al*, *A&A* **518** 100 (2010).
- [3] Schuller, F., Menten, K. M., Contreras, Y., *et al*, *A&A* **504** 415 (2009).
- [4] Lada, C. J. & Lada, E. A. *ARA&A* **41** 57 (2003).
- [5] Dame, T., Hartmann, D., & Thaddeus, P. *ApJ* **547** 792 (2001).
- [6] Jackson, J., Rathborne, J. M., Shah, R. Y., *et al*, *ApJS* **163** 145 (2006).
- [7] Barnes, P. J., Yonekura, Y., Fukui, Y., *et al*, *ApJS* **196** 12 (2011).
- [8] Jackson, J. M., Rathborne, J. M., Foster, J. B., *et al*, *PASA* **30** 57 (2013).
- [9] Barnes, P. J., Muller, E., Indermuehle, B., *et al*, *ApJ* **812** 6 (2015).
- [10] Schuller, F., Csengeri, Urquhart, J. S., *et al*, *A&A*, accepted (2017).
- [11] Umemoto, T. *et al*, this volume (2017).
- [12] Yonekura, Y., Fukui, Y., *et al*, unpublished.
- [13] Narayanan, D., Cox, T. J., Shirley, Y., *et al*, *ApJ* **684** 996 (2008).

[14] Schap, W. J. III, Barnes, P. J., Ordonez, A., *et al*, *MNRAS* **465** 2559 (2016).

[15] Barnes, P. J., Ryder, S. D., O’Dougherty, S. N., *et al*, *MNRAS* **432** 2231 (2013).

[16] Barnes, P. J., Hernandez, A. K., O’Dougherty, S. N., *et al*, *ApJ* **831** 67 (2016).